

Surface location of sodium atoms attached to ^3He nanodroplets

F. Stienkemeier,¹ O. Bünermann,¹ R. Mayol,² F. Ancilotto,³ M. Barranco,² and M. Pi²

¹*Fakultät für Physik, Universität Bielefeld, D-33615 Bielefeld, Germany*

²*Departament E.C.M., Facultat de Física, Universitat de Barcelona, E-08028, Spain*

³*INFN (Udr Padova and DEMOCRITOS National Simulation Center,*

Trieste, Italy) and Dipartimento di Fisica “G. Galilei”,

Università di Padova, via Marzolo 8, I-35131 Padova, Italy

(Dated: November 1, 2018)

We have experimentally studied the electronic $3p \leftarrow 3s$ excitation of Na atoms attached to ^3He droplets by means of laser-induced fluorescence as well as beam depletion spectroscopy. From the similarities of the spectra (width/shift of absorption lines) with these of Na on ^4He droplets, we conclude that sodium atoms reside in a “dimple” on the droplet surface. The experimental results are supported by Density Functional calculations at zero temperature, which confirm the surface location of sodium on ^3He droplets, and provide a microscopic description of the “dimple” structure.

PACS numbers: 68.10.-m , 68.45.-v , 68.45.Gd

Detection of laser-induced fluorescence (LIF) and beam depletion (BD) signals upon laser excitation provides a sensitive spectroscopic technique to investigate electronic transitions of chromophores attached to ^4He nanodroplets [1]. While most of atomic and molecular dopants migrate to the center of the droplet, alkali atoms (and alkaline earth atoms to some extent [2]) have been found to reside on the surface of ^4He droplets, as evidenced by the much narrower and less shifted spectra when compared to those found in bulk liquid ^4He [3, 4, 5, 6]. This result has been confirmed by Density Functional (DF) [7] and Path Integral Monte Carlo (PIMC) [8] calculations, which predict surface binding energies of a few Kelvin, in agreement with the measurements of detachment energy thresholds using the free atomic emissions [9]. The surface of liquid ^4He is only slightly perturbed by the presence of the impurity, which produces a “dimple” on the underlying liquid. The study of these states can thus provide useful information on surface properties of He nanodroplets complementary to that supplied by molecular-beam scattering experiments [10, 11].

Although the largest amount of work has been devoted to the study of pure and doped ^4He nanodroplets -see [12, 13] and Refs. therein-, the only neutral Fermi systems capable of being observed as bulk liquid and droplets are made of ^3He atoms, and for this reason they have also attracted the interest of experimentalists and theoreticians [11, 14, 15, 16, 17, 18]. We recall that while ^4He droplets, which are detected at an experimental temperature (T) of ~ 0.38 K, are superfluid, these containing only ^3He atoms, even though detected at a lower T of ~ 0.15 K, do not exhibit superfluidity [19].

The behavior of molecules in He clusters is especially appealing. In particular, probes at the surface of the droplets are desirable because they allow to investigate the liquid–vacuum interface as well as droplet surface excitations. The latter are of interest in the comparison of the superfluid vs. normal fluid behavior, particularly because the Bose–Einstein condensate fraction has been

calculated to approach 100% on the surface of ^4He [20]. Small ^3He drops are difficult to detect since, as a consequence of the large zero-point motion, a minimum number of atoms is needed to produce a selfbound drop [15]. Microscopic calculations of ^3He droplets are scarce, and only concern the ground state structure [15, 18]. Ground state properties and collective excitations of ^3He droplets doped with some inert atoms and molecular impurities have been addressed within the Finite Range Density Functional (FRDF) theory [17], that has proven to be a valuable alternative to Monte Carlo methods, which are notoriously difficult to apply to Fermi systems. Indeed, a quite accurate description of the properties of inhomogeneous liquid ^4He at $T = 0$ has been obtained within DF theory [21], and a similar approach has followed for ^3He (see [17, 22] and Refs. therein).

The experiments we report have been performed in a helium droplet machine used earlier for LIF and BD studies, and is described elsewhere [2]. Briefly, helium gas is expanded under supersonic conditions from a cold nozzle forming a beam of droplets traveling freely under high vacuum conditions. The droplets are doped downstream employing the pick-up technique: in a heated scattering cell, bulk sodium is evaporated in such a way that, on average, a single metal atom is carried by each droplet. LIF absorption spectra of doped droplets are recorded upon electronic excitation using a continuous wave ring-dye laser and detection in a photo multiplier tube (PMT). Since electronic excitation of alkali-doped helium droplets is eventually followed by desorption of the chromophore, BD spectra can be registered by a Langmuir-Taylor surface ionization detector [23] housed in a separate ultra-high vacuum chamber. Phase-sensitive detection with respect to the chopped laser or droplet beam was used. For that reason the BD signal (cf. Fig. 2), i.e. a decrease in intensity, is directly recorded as a positive yield. For these experiments, a new droplet source was built to provide the necessary lower nozzle temperatures to condense ^3He droplets. Expanding $P_0 = 20$ bar of helium gas through a nozzle $5 \mu\text{m}$

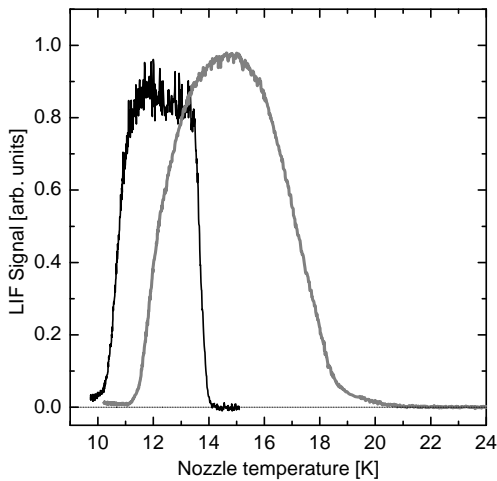


FIG. 1: Laser-induced fluorescence signal as a function of nozzle temperature forming ${}^3\text{He}$ droplets (black) in comparison to ${}^4\text{He}$ droplets (grey). In both runs a stagnation pressure of 20 bar was used; nozzle diameter was $5\ \mu\text{m}$. Normalization is such that the plot gives the correct relative intensities.

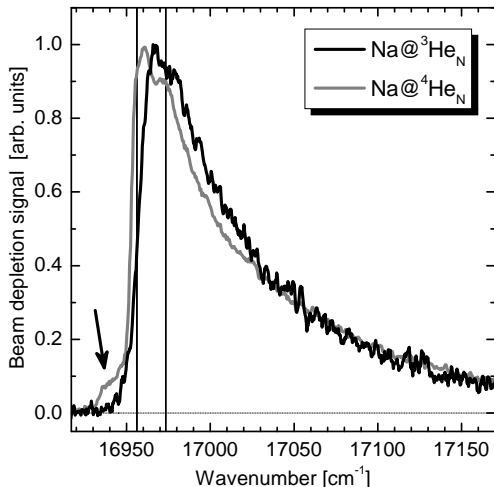


FIG. 2: Beam depletion spectra of Na atoms attached to ${}^3\text{He}/{}^4\text{He}$ nanodroplets. The vertical lines indicate the positions of the two components of the Na gas-phase $3p \leftarrow 3s$ transition.

in diameter, we now can establish temperatures down to 7.5 K using a two-stage closed cycle refrigerator (Sumitomo Heavy Industries, Model: RDK-408D). In this way, without needing any liquid helium or nitrogen for pre-cooling or cold shields, stable beam conditions can be utilized over several days.

Fig. 1 compares the number of Na-doped ${}^3\text{He}$ vs. ${}^4\text{He}$ droplets expanding 20 bar helium as a function of the nozzle temperature T_0 . The absolute number densities in the maxima of both distributions are quite similar. For the spectroscopic measurements presented in the following, we set $T_0 = 11\ \text{K}$ for ${}^3\text{He}$, and $T_0 = 15\ \text{K}$ for ${}^4\text{He}$. These conditions are expected to result in comparable mean cluster sizes around 5000 atoms per droplet [11, 24]. In

Fig. 2 the absorption spectrum of Na atoms attached to ${}^3\text{He}$ nanodroplets is shown in comparison to Na-doped ${}^4\text{He}$ droplets. We present here the BD spectra because they do not contain the strong fluorescence background lines of free Na atoms which cover the crucial steep increase of the droplet spectrum. Moreover, LIF does not always represent the total absorption spectrum because it relies on the emission of a photon in the spectral range of the PMT. Hence, absorption processes followed by either radiationless decay or emission of photons in the infrared spectral region are suppressed. The latter has been observed in LIF spectra where alkali-helium exciplexes form upon excitation of alkali atoms on the surface of ${}^4\text{He}$ droplets [5, 25]. In our experiment Na ${}^3\text{He}$ exciplexes are formed in the same way as their Na ${}^4\text{He}$ counterparts. This became immediately obvious because we were able to discriminate the corresponding red-shifted emission intensities. Furthermore, we followed directly the Na ${}^3\text{He}$ formation in real-time applying femtosecond techniques. These results will be presented in a forthcoming paper [26]. However, as far as the measured absorption spectra of Na@ ${}^3\text{He}_N$ are concerned, the LIF data are very well in accord with the BD absorption.

The outcome of the spectrum of Na attached to ${}^3\text{He}$ nanodroplets is very similar to the spectrum on ${}^4\text{He}$ droplets, which is remarkable for two apparently very different fluids -one normal and the other superfluid-, and confirms immediately the surface location: embedded atoms are known to evolve large blue-shifts of the order of a couple of hundreds of wavenumbers and much more broadened absorption lines, like e.g. observed experimentally in bulk helium [27]. The blue shift is a consequence of the repulsion of the helium environment against the spatially enlarged electronic distribution of the excited state (“bubble effect”). The interaction towards the ${}^3\text{He}$ droplets appears to be slightly enhanced, evidenced by the small extra blue shift of the spectrum compared to the ${}^4\text{He}$ spectrum. In a simple picture this means that more helium atoms are contributing or, in other words, a more prominent dimple interacts with the chromophore. The upper halves of the spectra come out almost identical, when shifting the ${}^3\text{He}$ spectrum $8\ \text{cm}^{-1}$ to lower frequencies. The increase in width (FWHM) of the spectrum is only 7% for ${}^3\text{He}$ droplets. Taking into account the narrowing of the absorption line for small helium droplets [3] and the uncertainty in the ${}^3\text{He}$ droplet size distribution, this difference might not even be significant. Although the width of the absorption might be hard to interpret, the blue shift is a clear indication that the “dimple” is more pronounced than in ${}^4\text{He}$ droplets. Regarding the substructure of the line, the only notable exception is the absence of the red-shifted shoulder, which is observed in the case of ${}^4\text{He}$ and marked with an arrow in Fig. 2. This feature, which is even more pronounced in the absorption of Li-doped ${}^4\text{He}$ droplets [3] has not been interpreted yet. The shift with respect to the maximum of the absorption line is $\approx 20\ \text{cm}^{-1}$, too high in energy to be attributed to an excited compres-

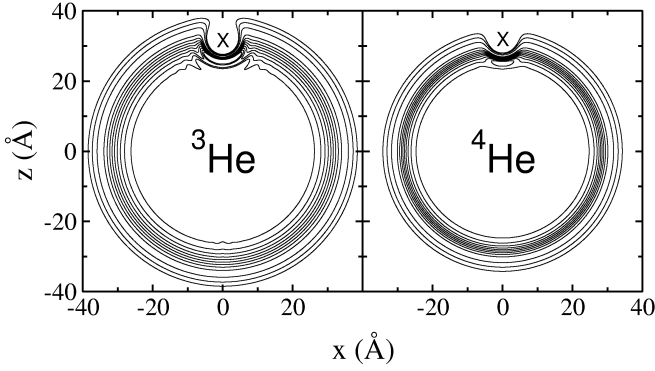


FIG. 3: Equidensity lines in the $x-z$ plane showing the stable state of a Na atom (cross) on a He_{2000} droplet. The 9 inner lines correspond to densities $0.9\rho_0$ to $0.1\rho_0$, and the 3 outer lines to $10^{-2}\rho_0$, $10^{-3}\rho_0$, and $10^{-4}\rho_0$ ($\rho_0 = 0.0163 \text{ \AA}^{-3}$ for ${}^3\text{He}$, and 0.0218 \AA^{-3} for ${}^4\text{He}$).

sional or surface mode of the droplet at 0.38 K [17, 28].

FRDF calculations at $T = 0$ confirm the picture emerging from the measurements just reported, i.e. the surface location of Na on ${}^3\text{He}$ nanodroplets causing a more pronounced “dimple” than in ${}^4\text{He}$ droplets. We have investigated the stable configurations of a sodium atom on both ${}^3\text{He}$ and ${}^4\text{He}$ clusters of different sizes. The FRDF’s used for ${}^3\text{He}$ and ${}^4\text{He}$ are described in [29], with the changes introduced in [30]. The large number of ${}^3\text{He}$ atoms we are considering allows to use the extended Thomas-Fermi approximation [16]. The minimization of the energy DF’s with respect to density variations, subject to the constraint of a given number of He atoms N , leads to Euler-Lagrange equations whose solution give the equilibrium particle densities $\rho(\mathbf{r})$. These equations have been solved as indicated in [31]. The presence of the foreign impurity is modeled by a suitable potential obtained by folding the helium density with a Na-He pair potential $V_{\text{He-Na}}$. Since the adsorption properties of weakly interacting atoms on liquid He are known to be very sensitive to the details of that potential, accurate descriptions of the impurity-He interactions are mandatory for quantitative predictions. We have used the potential proposed by Patil [32]. Potential energy curves describing the He-alkali interaction have been calculated by ab-initio methods [8], and found to agree very well with the Patil potential.

Fig. 3 shows the equilibrium configuration for a Na atom adsorbed onto He_{2000} clusters. For a given N , the size of the ${}^3\text{He}_N$ droplet is larger than that of the ${}^4\text{He}_N$ droplet -an obvious consequence of the smaller ${}^3\text{He}$ saturation density-. Comparison with the stable state on the ${}^4\text{He}_{2000}$ cluster shows that, in agreement with the experimental findings presented before, the “dimple” structure is more pronounced in the case of ${}^3\text{He}$, and that the Na impurity lies *inside* the surface region for ${}^3\text{He}$ and *outside* the surface region for ${}^4\text{He}$ [33]. We attribute this to the lower surface tension of ${}^3\text{He}$ (0.113 K/\AA^2) as compared to that of ${}^4\text{He}$ (0.274 K/\AA^2), which also makes the surface

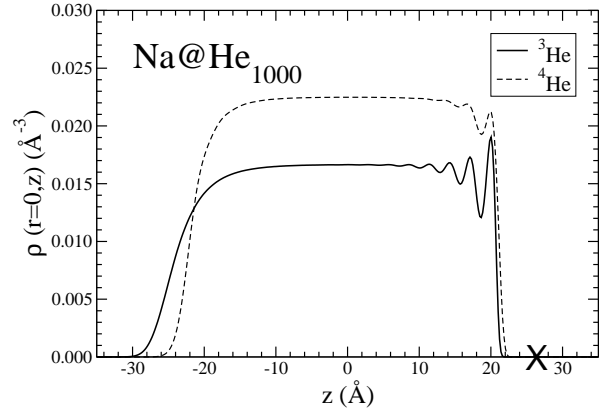


FIG. 4: Density profiles along a line connecting the impurity to the center of the cluster showing the equilibrium configuration of a Na atom (cross) on He_{1000} nanodroplets.

thickness of bulk liquid and droplets larger for ${}^3\text{He}$ than for ${}^4\text{He}$ [10, 11]. The Na-droplet equilibrium distance, here defined as the ‘radial’ distance between the impurity and the point where the density of the pure drop would be $\rho \sim \rho_0/2$ (ρ_0 being the saturation density of bulk liquid He), is $R \sim 1.1 \text{ \AA}$ for ${}^3\text{He}$, and $R \sim 3.6 \text{ \AA}$ for ${}^4\text{He}$. For the larger droplets we have studied, R is nearly N -independent. A related quantity is the deformation of the surface upon Na adsorption, which can be characterized [7] by the dimple depth, ξ , defined as the difference between the position of the dividing surface at $\rho \sim \rho_0/2$, with and without impurity, respectively. We find $\xi = 4.4 \text{ \AA}$ for ${}^3\text{He}$, and $\xi = 1.8 \text{ \AA}$ for ${}^4\text{He}$.

Fig. 4 shows the density profiles for Na@He_{1000} . Note the more diffuse liquid-vacuum interface for the ${}^3\text{He}$ droplet far from the impurity, and the occurrence of more marked density oscillations (with respect to the ${}^4\text{He}$ case) where the softer ${}^3\text{He}$ surface is compressed by the adsorbed Na atom. Our calculations thus provide a detailed picture of the He structure around the impurity, which is an essential ingredient for any line-shape calculation of the main electronic transitions in the adatom [3].

Solvation energies defined as

$$S_{Na} = E(\text{Na@He}_N) - E(\text{He}_N) \quad (1)$$

are shown in Fig. 5. To compare with “exact” PIMC result [8], we have calculated $\text{Na@}{}^4\text{He}_{300}$. Part of the small difference between the two values has to be attributed to our neglecting of the zero-point energy of Na.

We have fitted the S_{Na} ’s to a mass formula of the kind

$$S_{Na}(N) = S_0 + \frac{S_1}{N^{1/3}} + \frac{S_2}{N^{2/3}} \quad (2)$$

and have found $S_0 = -12.1(-12.5)$, $S_1 = -28.3(-31.6)$, and $S_2 = 37.3(37.6) \text{ K}$ for ${}^4\text{He}({}^3\text{He})$. The lines in Fig. 5 are the result of the fit. The value $S_{Na} \sim -12 \text{ K}$ has been obtained within FRDF theory for Na adsorbed on the *planar* surface of ${}^4\text{He}$ [7], which would correspond to the $N = \infty$ limit in Fig. 5.

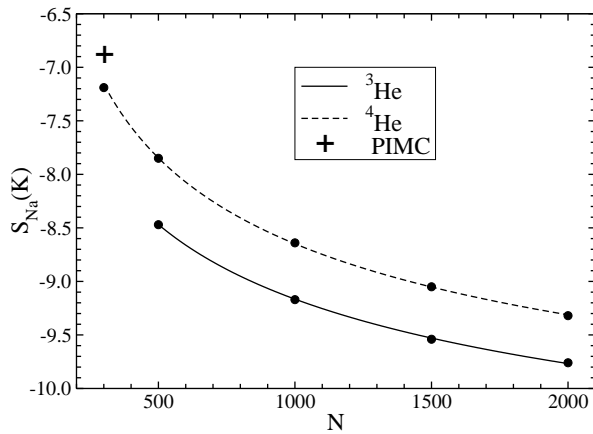


FIG. 5: Na solvation energy as a function of the cluster size. The cross is the PIMC result of [8].

In conclusion, the presented experimental and theoretical results show that alkali adsorption on ^3He droplets occurs in very much the same way as in the case of ^4He , i.e. the adatom is located on the surface in a slightly more pronounced “dimple”. Our calculations provide a microscopic description of the liquid structure around the impurity, which is a necessary input for any line-shape calculation as well as for the understanding of dynamical processes which already have been observed in time-dependent experiments [26].

We thank Flavio Toigo for useful comments. This work has been performed under grants MIUR-COFIN 2001 (Italy), BFM2002-01868 from DGI (Spain), and 2001SGR-00064 from Generalitat of Catalunya. Financial support by the Deutsche Forschungsgemeinschaft (Germany) is gratefully acknowledged.

-
- [1] F. Stienkemeier and A.F. Vilesov, *J. Chem. Phys.* **115**, 10119 (2001).
- [2] F. Stienkemeier, F. Meier, and H. O. Lutz, *J. Chem. Phys.* **107**, 10816 (1997); *Eur. Phys. J. D* **9**, 313 (1999).
- [3] F. Stienkemeier et al., *Z. Phys. D* **38**, 253 (1996).
- [4] F. Stienkemeier et al., *J. Chem. Phys.* **102**, 615 (1995);
- [5] C. Callegari et al., *J. Phys. Chem.* **102**, 95 (1998).
- [6] F. Brühl, R. Trasca, and W. Ernst, *J. Chem. Phys.* **115**, 10220 (2001).
- [7] F. Ancilotto et al., *Z. Phys. B* **98**, 323 (1995).
- [8] A. Nakayama and K. Yamashita, *J. Chem. Phys.* **114**, 780 (2001).
- [9] J. Reho et al., *Faraday Discuss* **108**, 161 (1997).
- [10] F. Dalfovo, J. Harms, and J.P. Toennies, *Phys. Rev. B* **58**, 3341 (1998).
- [11] J. Harms et al., *Phys. Rev. B* **63**, 184513 (2001).
- [12] J.P. Toennies and A.F. Vilesov, *Annu. Rev. Phys. Chem.* **49**, 1 (1998); K.K. Lehmann and G. Scoles, *Science* **279**, 2065 (1998); J.P. Toennies, A.F. Vilesov, and K.B. Whaley, *Physics Today* **54**, 31 (2001).
- [13] C. Callegari et al., *Phys. Rev. Lett.* **83**, 5058 (1999); **84**, 1848(E) (2000); Y. Kwon et al., *J. Chem. Phys.* **113**, 6469 (2000); E.W. Draeger and D.M. Ceperley, *Phys. Rev. Lett.* **90**, 65301 (2003).
- [14] J. Harms et al., *J. Mol. Spectrosc.* **185**, 204 (1997).
- [15] V.R. Pandharipande, S.C. Pieper, and R.B. Wiringa, *Phys. Rev. B* **34**, 4571 (1986).
- [16] S. Stringari and J. Treiner, *J. Chem. Phys.* **87**, 5021 (1987).
- [17] F. Garcias et al., *J. Chem. Phys.* **108**, 9102 (1998); *ibid* **115**, 10154 (2001).
- [18] R. Guardiola, *Phys. Rev. B* **62**, 3416 (2000).
- [19] S. Grebenev, J.P. Toennies, and A.F. Vilesov, *Science* **279**, 2083 (1998).
- [20] A. Griffin and S. Stringari, *Phys. Rev. Lett.* **76**, 259 (1996); E.W. Draeger and D.M. Ceperley, *ibid.* **90**, 65301 (2003).
- [21] F. Dalfovo et al., *Phys. Rev. B* **52**, 1193 (1995).
- [22] E.S. Hernández and J. Navarro, in *Microscopic Approaches to Quantum Liquids in Confined Geometries*, E. Krotscheck and J. Navarro Eds. pag. 261 (World Sci., Singapore, 2002).
- [23] F. Stienkemeier et al., *Rev. Sci. Instr.* **71**, 3480 (2000).
- [24] J. Harms and J. P. Toennies, unpublished results.
- [25] J. Reho et al., *J. Chem. Phys.* **113**, 9686 (2000).
- [26] O. Bünermann et al., unpublished (2003).
- [27] Y. Takahashi et al., *Phys. Rev. Lett.* **71**, 1035 (1993).
- [28] S.A. Chin and E. Krotscheck, *Phys. Rev. B* **45**, 852 (1992); *ibid.* **52**, 10405 (1995).
- [29] M. Barranco et al., *Phys. Rev. B* **56**, 8997 (1997).
- [30] R. Mayol et al., *Phys. Rev. Lett.* **87**, 145301 (2001).
- [31] M. Barranco et al., *Phys. Rev. B* **68**, 024515 (2003).
- [32] S.H. Patil, *J. Chem. Phys.* **94**, 8089 (1991).
- [33] The surface region is usually defined as that comprised between the radii at which $\rho = 0.1\rho_0$ and $\rho = 0.9\rho_0$, where ρ_0 is the He saturation density [10, 11, 16].